



Robust and Objective Evaluation of Superficial Punctate Keratopathy in a Murine Dry Eye Model

Hiroki Fujii, MD,¹ Kazuko Saeki, PhD,¹ Sujin Hoshi, MD, PhD,² Yuri Kadoya, MD,³ Tetsuro Oshika, MD, PhD,² Takehiko Yokomizo, MD, PhD¹

Purpose: To establish a robust and objective method to evaluate (SPK) superficial punctate keratopathy in a murine dry eye model by developing a reliable photographic system.

Design: Experimental study.

Subjects: A murine dry eye model was generated by exorbital lacrimal gland excision. Sham-operated mice were used as healthy controls. For the sham operation, an incision was made without touching the gland.

Methods: A photographic system was constructed, consisting of an LED lamp and a digital camera fitted with a zoom lens and sharp cut filter. SPK was detected by applying fluorescein solution. To validate the system, SPK was compared between dry eye mice and healthy control mice, and diquafosol (DIQUAS ophthalmic solution 3%; Santen Pharmaceutical Co., Ltd.) or cyclosporine (PAPILOCK Mini ophthalmic solution 0.1%; Santen Pharmaceutical Co., Ltd.) was used to dry eye mice.

Main Outcome Measures: SPK was evaluated using the parameters of fluorescence score and fluorescein-stained area.

Results: The photographs clearly indicated SPK in dry eye mice. A fluorescence score of 0 to 9 could be easily assessed, and the fluorescein-stained area was quantifiable. The fluorescein-stained area correlated with fluorescence score (correlation coefficient: 0.98), with good interobserver reliability (intraclass correlation coefficient: 0.999). The fluorescein-stained area increased significantly in dry eye mice compared with that of healthy controls ($P < 0.0001$). Both types of therapeutic eye drops decreased the fluorescein-stained area relative to saline-treated mice ($P < 0.05$ in diquafosol vs. saline; $P < 0.01$ in cyclosporine vs. saline).

Conclusions: This newly developed system is a robust alternative for quantitative evaluation of SPK in a murine dry eye model.

Financial Disclosure(s): Proprietary or commercial disclosure may be found in the Footnotes and Disclosures at the end of this article. *Ophthalmology Science* 2024;4:100414 © 2023 by the American Academy of Ophthalmology. This is an open access article under the CC BY-NC-ND license (<http://creativecommons.org/licenses/by-nc-nd/4.0/>).



Supplemental material available at www.aaojournal.org.

Dry eye disease (DED) is a disease of the ocular surface accompanied by ocular discomfort¹ with an estimated prevalence of 5% to 50% of the population.² DED and digital screen use are closely related.³ Screen time use has increased internationally,⁴ suggesting the incidence of DED will continue to increase.

Eyedrop preparations are available to alleviate DED. However, the pathogenesis of DED is so complex that “the management of DED remains something of an art.”⁵ Further basic and translational research are required to investigate the pathogenesis of DED and develop novel treatments. For basic and translational DED research, studies using multiple species of mammals have contributed to our understanding of DED. Among model animals, mice are useful because they are inexpensive, easy to handle, and genetic manipulations are generally performed in mice.⁶

The 2 primary murine DED models are the lacrimal gland excision model and the desiccating environmental stress model. Both models develop superficial punctate keratopathy (SPK), a major symptom of DED. SPK is generally detected with corneal fluorescein staining (CFS). Slit lamp microscopy can be used to evaluate SPK in humans, but no instrumentation can effectively evaluate the condition in mice. Currently, slit lamp microscopes^{7,8} and fluorescence stereo microscopes^{9,10} are the primary means used to evaluate SPK in mice, but both modalities are problematic.

Slit lamp microscopes require training for effective use.¹¹ They are expensive and immovable, making continuous observation impossible in some settings, because slit lamps cannot repeatedly be moved into specific pathogen-free (SPF) environments where experimental animals are

housed.¹² For research, it is essential to use the same illumination settings for all images,¹³ and the light source angle is often set to oblique in slit lamp microscopes.¹⁴ Mice have steeper corneas than do humans, which can easily cause a shadow artifact to be cast by incident light with an oblique angle. Shadow artifacts preclude precise evaluation of SPK. Moreover, most slit lamp microscope lenses have a shallow depth of field because they do not have a diaphragm, which compromises the ability to focus on the entire murine corneal area.

Fluorescence stereomicroscopes are also costly and immovable like slit lamp microscopes. Previous reports have utilized images of SPK taken by fluorescence stereomicroscopes.^{9,10} SPK lesions have a size of approximately 20 μm ,¹⁵ such that the fluorescence image should be a dot-like pattern image, with high contrast between the fluorescein-stained area and the non-stained area. However, previous SPK images captured by fluorescence stereomicroscopes were low-contrast, and, thus, SPK could not be detected clearly.^{9,10} Unclear fluorescent images result in unreliable evaluation of SPK. Therefore, commonly used instrumentation cannot clearly detect SPK in murine DED models.

An additional barrier for the evaluation of SPK in murine DED models is that the scoring systems used to evaluate SPK are subjective and observer dependent. In clinical DED, CFS methodology is well-established,¹⁶ and severity scores are relatively consistent between observers trained in ophthalmology.¹⁷ On the other hand, no method has been established to detect SPK in murine DED models. Further, observers quantifying SPK in basic research studies are commonly nonophthalmologists, so developing an objective evaluation system for this setting presents additional challenges.

Quantitative evaluation generally improves objectivity. In humans, prior studies have reported methods to evaluate SPK quantitatively based on digital images.^{14,18,19} In murine models, few reports have attempted quantitative evaluation.^{20,21} However, these reports analyzed only the central cornea, as the peripheral cornea was not pictured clearly due to the steepness of the cornea. Superficial punctate keratopathy often develops in limited zones of the cornea in humans²² and mice (Fig S1, available at www.ophthalmologyscience.org). Thus, analysis of the central cornea only cannot precisely evaluate DED severity.

For these backgrounds, a photographic system capable of focusing on the entirety of the cornea is essential, and objective quantitative measurement of SPK is necessary in a murine DED model. The purpose of the present study was to establish a photographic system that focuses on all zones of the cornea and determine whether SPK can be evaluated robustly and quantitatively measured in a murine DED model using this system.

Methods

Photographic System for Detecting SPK in a Murine DED Model

A photographic system was built with an LED lamp (IHR-LE90C100-AB; Leimac Ltd), a sharp cut filter (Y-52; HOYA

GROUP Optics Division), and a digital camera with an integrated display (AR-MC200HD; Armssystem Co, Ltd) fitted with a zoom lens (SDS-M19; Shodensha, Inc). The lens was affixed with a ring adapter (RA-28; Shodensha, Inc) and a protective filter (MC-28; Shodensha, Inc). The sharp cut filter was placed between the lens and the protective filter. An image of the instrument is shown in Figure 2.

Experimental Animals

Animal experiments were conducted according to the Association for Research in Vision and Ophthalmology Statement on the Use of Animals in Ophthalmic and Vision research and approved by the Ethics Committees for Animal Experiments of Juntendo University School of Medicine (Approval number 2023209). Female C57BL/6J mice aged 6 weeks were obtained from Oriental Yeast Co, Ltd and originated from The Jackson Laboratory. The mice were housed in an animal facility with SPF conditions and allowed free access to food and water.

Corneal Fluorescein Staining

Mice were anesthetized by intraperitoneal administration of ketamine hydrochloride (Ketalar for Intravenous Injection; Daiichi Sankyo Company, Limited; 100 mg/kg) and xylazine hydrochloride (Sigma-Aldrich Japan; 10 mg/kg). 0.5 μL of a 0.25% fluorescein solution (Fluorescein sodium salt; Sigma-Aldrich Co) was applied to the eye, and excess fluorescein was cleared with careful manual blinks. After 90 to 180 seconds following fluorescein application, corneal images were captured, and SPK was evaluated.

Evaluation of Corneal Scoring

Fluorescence score was evaluated as previously described.^{8,23} Briefly, each cornea was divided into 3 areas (upper, intermediate, and lower). Fluorescence score was categorized from 0 to 3 (0: no fluorescence, 1: fluorescence resembling sparse dots, 2: dense dot-like pattern, and 3: very dense dot-like fluorescence) on each area. Each score was added together for the entire eye (minimum score; 0 and maximum score; 9; higher scores indicate severe SPK).

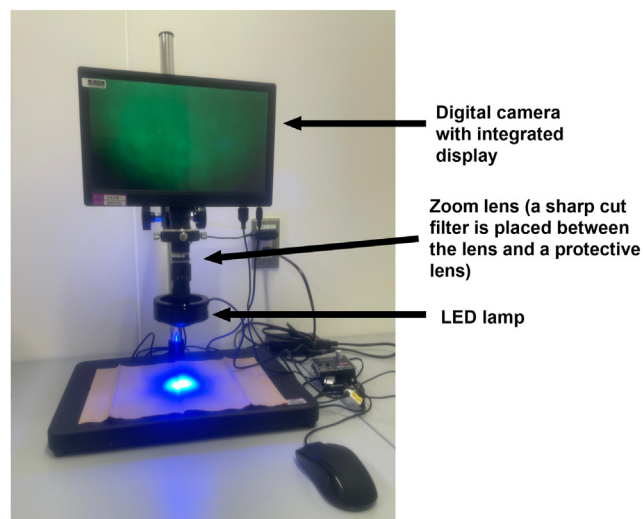


Figure 2. Appearance of the instrument.

Digital Image Analysis

Images were analyzed using ImageJ 1.54d software (<https://imagej.nih.gov/ij/>); provided in the public domain by the National Institution of Health) as previously described^{9,14} with slight modifications. The original image was opened in ImageJ, and the green channel image was split from the original image. The oval selections tool or the elliptical selections tool was used to set the range of interest (ROI) of the total corneal area. The percentage of the fluorescein-stained area was calculated under the same threshold in all images. This method eliminates artificial light reflection of the central corneal area by setting a threshold in ImageJ and removes the tear meniscus area by setting the ROI so that it does not include the tear meniscus area. Example images in each procedure are shown in Fig S3 (available at www.ophtalmologyscience.org).

DED Model

Unilateral (right side) exorbital lacrimal gland (ELG) excision was performed as previously described,^{7,8,23,24} with slight modifications. Briefly, mice were anesthetized by intraperitoneal ketamine/xylazine injection. Tarivid ophthalmic ointment (Santen Pharmaceutical Co, Ltd) was applied to the cornea before surgery to prevent drying. A skin incision was made on the temporal side to expose and remove the ELG. The skin incision was then sutured using 6-0 nylon sutures (MANI, Inc). Tarivid ophthalmic ointment was applied onto the incision to avoid bacterial infection.

Sham-operated Animals

Sham-operated mice were used as healthy controls and were compared with ELG excision-operated mice. For the sham operation, an incision was made unilaterally in the same zone without touching the ELG. Seven days after surgery, the fluorescein-stained area was evaluated.

Therapeutic Protocols

To verify that our system can detect the therapeutic effects of previously developed DED therapeutics, we used 2 protocols (saline vs. diquafosol, saline vs. cyclosporine) with different application frequencies and durations. Diquafosol ophthalmic solution was developed for DED treatment,^{25,26} and has utility in some clinic contexts including Japan.^{27–29} Cyclosporine alleviates DED via a different mechanism than diquafosol,^{30,31} and is approved by the United States Food and Drug Administration³⁸ and the European Medicines Agency.³² The details of each protocol are described below.

Saline Versus Diquafosol

On day 0 (preoperation), CFS was performed and the fluorescein-stained area was calculated. Mice then underwent ELG excision to induce DED. On day 7, CFS was again performed, and the fluorescein-stained area was calculated again. Mice were then assigned to 3% diquafosol solution (DIQUAS ophthalmic solution 3%; Santen Pharmaceutical Co, Ltd) or saline treatment (Otsuka Pharmaceutical Co, Ltd) treated group. The application frequencies and durations were determined based on those of a prior study,²⁶ with slight modifications. Mice received 5 μ L of the eye drop preparation 6 times daily in the right eye from days 8 to 14, then days 16 to 22. CFS was performed and the fluorescein-stained area was calculated on day 15 and day 23. Mice that developed significant ocular diseases other than DED in response to ELG excision (corneal infiltrate, corneal ulcer, filamentary keratitis, and

severe cataract) were excluded from analyses. Mice without sufficient SPK on day 7 were also excluded.

Saline Versus Cyclosporine

On day 0 (preoperation), CFS was performed and the fluorescein-stained area was calculated. Mice were then subjected to ELG excision to induce DED. On day 7, CFS was performed and the fluorescein-stained area was calculated again. Mice were randomized to receive cyclosporine (PAPILOCK Mini ophthalmic solution 0.1%; Santen Pharmaceutical Co, Ltd., <https://www.rad-ar.or.jp/siori/english/search/result?n=914&plain=1>) or saline treatment. The application frequencies and durations were determined based on those of a prior study,³¹ with slight modifications. Mice received 5 μ L of the eye drop 4 times daily from days 8 to 12, then days 14 to 16. CFS was performed and the fluorescein-stained area was calculated on day 13 and 17. Mice that developed significant ocular diseases other than DED in response to ELG excision (corneal infiltrate, corneal ulcer, filamentary keratitis, and severe cataract) were excluded from analyses. Mice without sufficient SPK on day 7 were also excluded.

Statistical Analysis

Statistical significance (*P* value) of changes in the fluorescein-stained area was determined with the Welch *t* test. Values are expressed as mean \pm SEM. One-sided *P* < 0.05 was considered statistically significant. The Pearson correlation value was used to evaluate the relationship between fluorescein-stained area and fluorescence score. Analyses were conducted with Prism 9 software (GraphPad Software). Intraclass correlation coefficients (ICC) in the fluorescence score and the fluorescein-stained area were calculated using EZR software, version 1.55 (Saitama Medical Center, Jichi Medical University) to determine the agreement between 2 examiners.

Results

Imaging Results Obtained Using This System

Using this system, we collected images of the murine cornea under white light and fluorescence images (Fig 2). The fixed light source provides excitation light perpendicular to the cornea. Additionally, it delivers a consistent intensity of excitation light (42 000 lx) to the cornea. Fluorescein was used at a concentration of “0.25%” because this concentration resulted in the highest signal-to-noise ratio in SPK images. Fluorescein has a peak excitation wavelength of 480 nm, a peak emission wavelength of 515 nm, and a stokes shift wavelength of 35 nm (Fig S4, available at www.ophtalmologyscience.org). A small stokes shift results in a decreased signal-to-noise ratio. This sharp cut filter improves the contrast between the fluorescein-stained area and nonstained area by selectively blocking light with wavelengths below 520 ± 5 nm. The zoom lens used in this system had a diaphragm, which allowed for the adjustment of the depth of field. Mice corneas are steeper than human corneas and, thus, require an improved depth of focus. In fact, a camera with an open diaphragm cannot focus on the entire corneal area, and, thus, SPK cannot be clearly detected in the peripheral cornea (Fig 5A, B). Adjusting the diaphragm allows focusing of the camera on the entire corneal surface (Fig 5C, D).

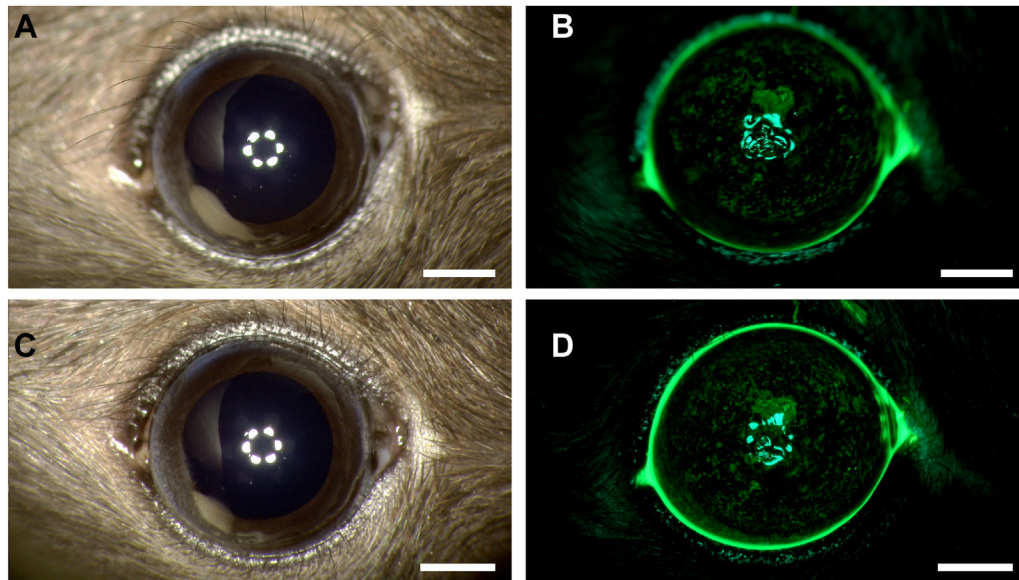


Figure 5. Images of a murine cornea using different diaphragm settings. **A**, Picture of a murine cornea focused on the corneal apex with an opened diaphragm (F-number: 6). **B**, Picture of superficial punctate keratopathy (SPK) with F-number: 6. **C**, Photograph of a murine cornea focused on the entire cornea with diaphragm adjustment (F-number: 12). **D**, Photograph of SPK with F-number: 12. Scale bar: 1 mm.

SPK Evaluation

The system clearly revealed the presence of SPK, which allowed the SPK score to be readily determined. Fluorescence scores are listed in Figure 6A.

The ICC of the score between a trained ophthalmologist (H.F; 5 years of clinic experience and 4 years of research experience in the ophthalmology field) and a nonspecialist (Y.K; no experience in the ophthalmologic field) was 0.89 (95% confidence interval: 0.736–0.947).

To analyze images and evaluate SPK quantitatively, the ROI was set for each image. Clear images allowed easy setting of the ROI. The fluorescein-stained area was then measured in the ROI. The ICC of the area was 0.999 (95% confidence interval: 0.992–1). The ICC of the fluorescein-stained area was better than that of the score, suggesting that quantitative evaluation of SPK was more objective. The fluorescein-stained area was correlated with scoring, with correlation coefficient equaling 0.98 (Fig 6B).

Comparison of the DED Model with Healthy Controls

The mean fluorescein-stained area was 23% in the sham-operated group and 49% in the ELG excision-operated group. The difference of SPK between the operated and sham groups could be compared using the new system, and the difference was statistically significant (Fig 7; $P < 0.0001$).

Effects of Eyedrop Treatments

In addition to making comparisons of SPK between DED and sham-operated mice, we examined the therapeutic efficacy of DED eyedrops in alleviating SPK. The graphic protocols are shown in Figure 8A, C. Both eyedrops

decreased the fluorescein-stained area more markedly than saline (Fig 8B, D). The difference was significant in the first evaluation time points ($P < 0.05$, saline vs. diquafosol day 15, $P < 0.01$, saline vs. cyclosporine day 13). This demonstrated that the newly developed system can be used to assess the therapeutic effects of treatment modalities.

Discussion

In the present study, we demonstrated that a newly developed imaging system can be used to evaluate SPK by CFS in the murine DED model. Moreover, images from the system were sufficiently clear for quantitative evaluation of SPK as the fluorescein-stained area. The value of the fluorescein-stained area was stable between examiners, with a high ICC between a trained ophthalmologist and a nonspecialist.

Current methods used to evaluate SPK, such as slit lamp microscopes and fluorescence stereomicroscopes, are limited by factors such as prohibitive cost and immovability. The system developed in the present study is portable, allowing continuous observation in SPF environments. The cost is ~10% that of commonly used instrumentation (approximately \$3100 vs. \$31000; conversion rate: 1 United States Dollar = 130 Japanese Yen). It was also assembled with existing parts such as a lens, lamp, and camera that are freely available and easy to operate.

Previous studies have also used instruments other than slit lamp microscopes and fluorescence stereomicroscopes to evaluate SPK in DED mice.^{12,23,24} However, these instruments cannot detect the presence and severity of SPK as reliably. Portable hand-held slit lamps²⁴ are easier to use than slit lamp microscopes but cannot record

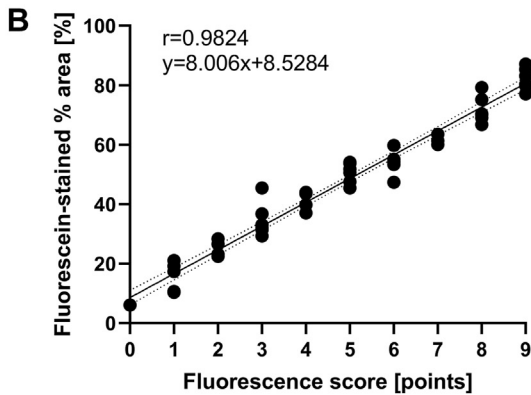
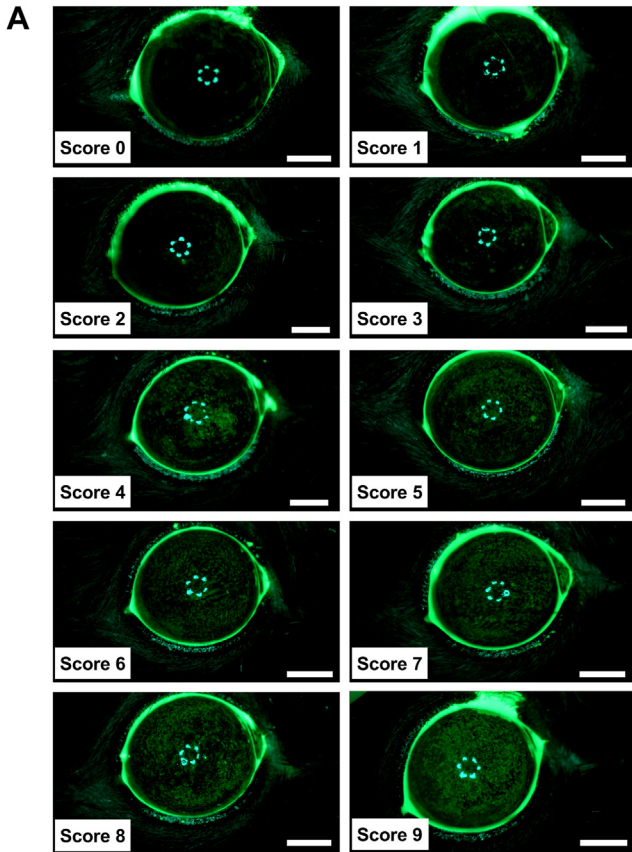


Figure 6. Fluorescence scores and fluorescein-stained areas. **A**, Corneal fluorescence score. Scale bar: 1 mm. **B**, Correlation between previous fluorescence score and fluorescein-stained area relative to entire cornea (%) measured with ImageJ. Pearson’s correlation coefficient was calculated ($r: 0.9824$). The fitted regression line (solid) is shown with a corresponding 95% confidence interval (dotted lines).

images. Digital cameras²³ are inexpensive and easy to operate but still require a high-quality lens and diaphragm to zoom into the corneas of mice, and to focus on all regions of the cornea. Further, the light source is assembled apart from the digital camera, which results in unstable evaluation because the irradiation angle of the light source and the distance between the light source and the cornea cannot be

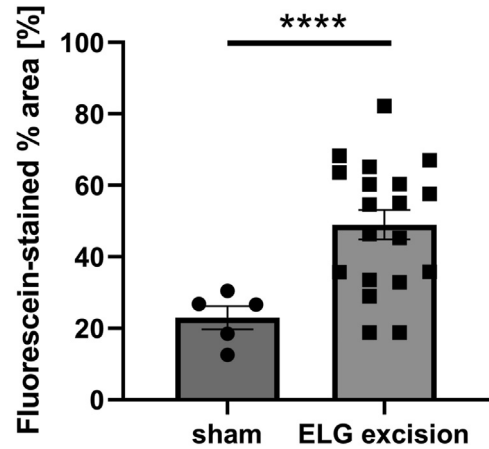


Figure 7. Murine dry eye disease model. Difference in fluorescein-stained area (% of total corneal area) between sham-operated mice and exorbital lacrimal gland (ELG) excision-operated mice (sham: $n = 5$; ELG excision: $n = 15$). The exact values of the fluorescein-stained area were 23.0 ± 3.27 and 49.0 ± 4.11 in the sham-operated group and ELG excision-operated group, respectively. **** $P < 0.0001$, Welch t test.

fixed for each sample. A prior study developed a device that can be connected to smartphones to capture images and videos of murine corneas.¹² This would be an ideal platform to image murine corneas as smartphones are nearly ubiquitous, but common smartphones, including the iPhone 7 used in the study, have a small F-number and cannot capture well-focused images of murine corneas. Additionally, holding the smartphone in-hand introduces difficulties in maintaining consistent shooting angle and distance, and the quality of the pictures is therefore not stable. The newly developed system overcomes these limitations, thus presenting additional benefits compared to these instruments as well.

The limitation of the study is that the definition of “total corneal area” in setting the ROI is indefinite, so ROI can be different among examiners. We set the ROI in a circular or elliptic form with a slight margin from the tear meniscus, and the number of pixels set as a margin was variable between users. Some studies set a fixed 2-mm diameter circle placed on the central cornea as the ROI.^{20,21} Another study set a circle with a diameter adjusted to the vertical corneal diameter.⁹ Each method can be used to set the same ROI independent of examiners. However, these methods might not analyze the noncentral areas of the cornea because the ROI is always set in a circular form. On the other hand, we set the ROI so that it covered the total corneal area in the form of an ellipse. We did not define the length of the margin from the tear meniscus when setting the ROI, which resulted in variability between examiners. Nevertheless, we identified a high ICC between examiners regardless of ophthalmology expertise.

Mice are a preferred animal model for basic and translational research. Mice are easy to handle, and the tear film lipids produced by meibomian glands are similar to that of humans.³³ Recently, the association between DED and

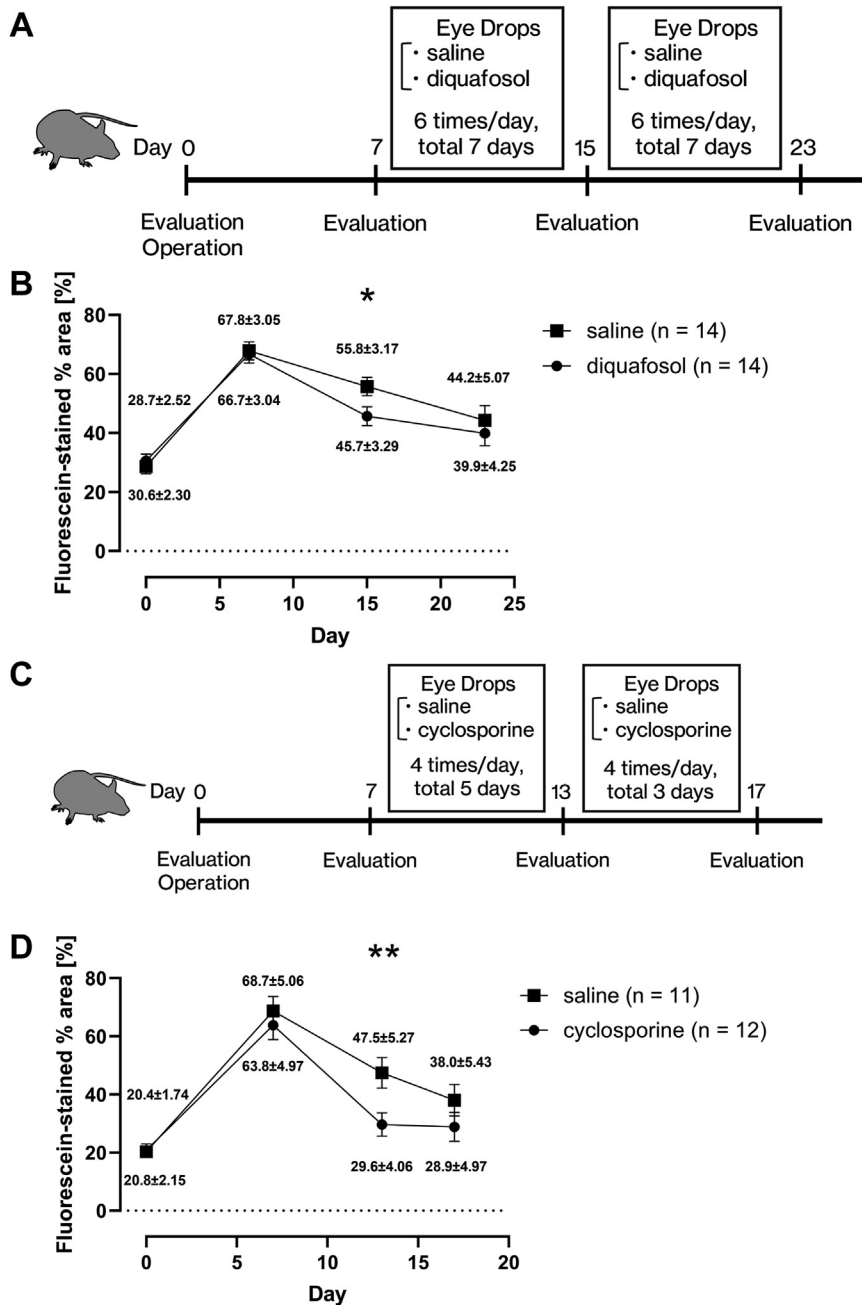


Figure 8. Assessment of therapeutic effects of dry eye disease. **A**, Graphic workflow of saline vs. diquafosol. **B**, Fluorescein-stained % area at each time point in saline vs. diquafosol protocol (n = 14/group). *P < 0.05, Welch t test. **C**, Graphic workflow of saline vs. cyclosporine. **D**, Fluorescein-stained % area at each time point in saline vs. cyclosporine protocol (saline: n = 11, cyclosporine: n = 12). **P < 0.01, Welch t test.

tear film lipids produced by meibomian glands has become a topic of investigation.^{34,35} Genes related to lipids produced by meibomian glands have protective effects in mouse DED.^{36,37} Murine DED models are extremely important for mechanistic studies involving transgenic animals, and the modality developed in the present study is expected to contribute to further research in the field. In conclusion,

the newly developed approach is a cost-effective and robust alternative for the evaluation SPK in murine dry eye.

Acknowledgments

The authors thank the members of our laboratory, Lewis Blevis, and Akira Matsuda for advice and helpful discussion. The authors also thank Yosuke Asada for technical assistance with

the surgical procedure and Satoshi Iwamoto for advice on CFS and evaluation of corneal scoring. The authors are grateful to the members of the Laboratory of Biomedical Research Resources, the Laboratory of Proteomics and Biomolecular Science, the

Laboratory of Morphology and Image Analysis, and the Laboratory of Molecular and Biochemical Research, Biomedical Research Core Facilities, Juntendo University Graduate School of Medicine, for technical assistance.

Footnotes and Disclosures

Originally received: June 28, 2023.

Final revision: September 25, 2023.

Accepted: October 13, 2023.

Available online: October 19, 2023. Manuscript no. XOPS-D-23-00153.

¹ Department of Biochemistry, Juntendo University Graduate School of Medicine, Bunkyo-ku, Tokyo, Japan.

² Department of Ophthalmology, Faculty of Medicine, University of Tsukuba, Tsukuba, Ibaraki, Japan.

³ Department of Obstetrics and Gynecology, Nippon Medical School Chiba Hokusoh Hospital, Chiba, Japan.

Disclosure(s):

All authors have completed and submitted the ICMJE disclosures form.

The authors have no proprietary or commercial interest in any materials discussed in this article.

This study was supported by a grant from Institute for Environmental & Gender-specific Medicine, Juntendo University (Chiba, Japan, grant number: E2107), a Grant-in-Aid (S1411007) for Special Research in Subsidies for ordinary expenses of private schools from The Promotion and Mutual Aid Corporation for Private Schools of Japan, and the Japan Agency for Medical Research and Development (grant number: JP19gm1210006). These funding organizations had no role in the design or conduct of this research.

HUMAN SUBJECTS: No human subjects were included in this study.

ANIMAL SUBJECTS: Animal experiments were conducted according to the Association for Research in Vision and Ophthalmology (ARVO) Statement on the Use of Animals in Ophthalmic and Vision research and approved by the Ethics Committees for Animal Experiments of Juntendo

University School of Medicine (Approval number 2023209). Female C57BL/6J mice aged 6 weeks were obtained from Oriental Yeast Co., Ltd. (Tokyo, Japan) and originated from The Jackson Laboratory. The mice were housed in an animal facility with SPF conditions and allowed free access to food and water.

Author Contributions:

Conception and design: Fujii, Saeki, Hoshi, Oshika, Yokomizo

Analysis and interpretation: Fujii, Saeki, Hoshi, Kadoya, Yokomizo

Data collection: Fujii, Saeki, Hoshi, Kadoya, Yokomizo

Obtained funding: N/A

Overall responsibility: Fujii, Saeki, Hoshi, Kadoya, Oshika, Yokomizo

This material is under consideration for presentation at the 43rd Annual Scientific Meeting of the Japanese Society of Ocular Pharmacology, Japan, November 2023.

Abbreviations and Acronyms:

CFS = corneal fluorescein staining; **DED** = dry eye disease; **ELG** = exorbital lacrimal gland; **ICC** = intraclass correlation coefficients; **ROI** = range of interest; **SPF** = specific pathogen-free; **SPK** = superficial punctate keratopathy.

Keywords:

Dry eye model, Superficial punctate keratopathy, Corneal fluorescein staining, Methodology.

Correspondence:

Takehiko Yokomizo, MD, PhD, Department of Biochemistry, Juntendo University Graduate School of Medicine, 2-1-1 Hongo, Bunkyo-ku, Tokyo 113-8421, Japan. E-mail: yokomizo-ky@umin.ac.jp.

References

- Craig JP, Nichols KK, Akpek EK, et al. TFOS DEWS II definition and classification report. *Ocul Surf*. 2017;15:276–283.
- Stapleton F, Alves M, Bunya VY, et al. TFOS DEWS II epidemiology report. *Ocul Surf*. 2017;15:334–365.
- Al-Mohtaseb Z, Schachter S, Shen Lee B, et al. The relationship between dry eye disease and digital screen Use. *Clin Ophthalmol*. 2021;15:3811–3820.
- DataReportal. Digital 2022 global digital overview. <https://datareportal.com/reports/digital-2022-global-overview-report>; 2022. Accessed June 20, 2023.
- Jones L, Downie LE, Korb D, et al. TFOS DEWS II management and therapy report. *Ocul Surf*. 2017;15:575–628.
- Huang W, Tourmouzis K, Perry H, et al. Animal models of dry eye disease: useful, varied and evolving (review). *Exp Ther Med*. 2021;22:1394.
- Stevenson W, Chen Y, Lee SM, et al. Extraorbital lacrimal gland excision: a reproducible model of severe aqueous tear-deficient dry eye disease. *Cornea*. 2014;33:1336–1341.
- Nakamura T, Hata Y, Nagata M, et al. JBP485 promotes tear and mucin secretion in ocular surface epithelia. *Sci Rep*. 2015;5:10248.
- Yamazaki R, Yamazoe K, Yoshida S, et al. The Semaphorin 3A inhibitor SM-345431 preserves corneal nerve and epithelial integrity in a murine dry eye model. *Sci Rep*. 2017;7:15584.
- Ziniauskaitė A, Ragauskas S, Hakkarainen JJ, et al. Efficacy of trabendoson in a mouse Keratoconjunctivitis Sicca (KCS) model for dry-eye syndrome. *Invest Ophthalmol Vis Sci*. 2018;59:3088–3093.
- Nelson JG, Stoimenova D, Quaday KA, et al. Labels improve emergency medicine physician comfort and ability to use a slit lamp. *AEM Educ Train*. 2021;5:e10570.
- Shimizu E, Ogawa Y, Yazu H, et al. “Smart Eye Camera”: an innovative technique to evaluate tear film breakup time in a murine dry eye disease model. *PLoS One*. 2019;14:e0215130.
- Bron AJ, Evans VE, Smith JA. Grading of corneal and conjunctival staining in the context of other dry eye tests. *Cornea*. 2003;22:640–650.
- Pellegrini M, Bernabei F, Moscardelli F, et al. Assessment of corneal fluorescein staining in different dry eye subtypes using digital image analysis. *Transl Vis Sci Technol*. 2019;8:34.
- Courrier E, Lepine T, Hor G, et al. Size of the lesions of superficial punctate keratitis in dry eye syndrome observed with a slit lamp. *Cornea*. 2016;35:1004–1007.

16. Yokoi N, Georgiev GA, Kato H, et al. Classification of fluorescein breakup patterns: a novel method of differential diagnosis for dry eye. *Am J Ophthalmol*. 2017;180:72–85.
17. Chun YS, Park IK. Reliability of 4 clinical grading systems for corneal staining. *Am J Ophthalmol*. 2014;157:1097–1102.
18. Chun YS, Yoon WB, Kim KG, Park IK. Objective assessment of corneal staining using digital image analysis. *Invest Ophthalmol Vis Sci*. 2014;55:7896–7903.
19. Amparo F, Wang H, Yin J, et al. Evaluating corneal fluorescein staining using a novel automated method. *Invest Ophthalmol Vis Sci*. 2017;58:BIO168–BIO173.
20. Zaheer M, Wang C, Bian F, et al. Protective role of commensal bacteria in Sjogren syndrome. *J Autoimmun*. 2018;93:45–56.
21. Wu Y, Wu J, Bu J, et al. High-fat diet induces dry eye-like ocular surface damages in murine. *Ocul Surf*. 2020;18:267–276.
22. Fenner BJ, Tong L. Corneal staining characteristics in limited zones compared with whole cornea documentation for the detection of dry eye subtypes. *Invest Ophthalmol Vis Sci*. 2013;54:8013–8019.
23. Shinomiya K, Ueta M, Kinoshita S. A new dry eye mouse model produced by exorbital and intraorbital lacrimal gland excision. *Sci Rep*. 2018;8:1483.
24. Mecum NE, Cyr D, Malon J, et al. Evaluation of corneal damage after lacrimal gland excision in male and female mice. *Invest Ophthalmol Vis Sci*. 2019;60:3264–3274.
25. Pendergast W, Yerxa BR, Douglass 3rd JG, et al. Synthesis and P2Y receptor activity of a series of uridine dinucleoside 5'-polyphosphates. *Bioorg Med Chem Lett*. 2001;11:157–160.
26. Fujihara T, Murakami T, Fujita H, et al. Improvement of corneal barrier function by the P2Y(2) agonist INS365 in a rat dry eye model. *Invest Ophthalmol Vis Sci*. 2001;42:96–100.
27. Takamura E, Tsubota K, Watanabe H, et al. A randomised, double-masked comparison study of diquafosol versus sodium hyaluronate ophthalmic solutions in dry eye patients. *Br J Ophthalmol*. 2012;96:1310–1315.
28. Gong L, Sun X, Ma Z, et al. A randomised, parallel-group comparison study of diquafosol ophthalmic solution in patients with dry eye in China and Singapore. *Br J Ophthalmol*. 2015;99:903–908.
29. Matsumoto Y, Ohashi Y, Watanabe H, et al. Efficacy and safety of diquafosol ophthalmic solution in patients with dry eye syndrome: a Japanese phase 2 clinical trial. *Ophthalmology*. 2012;119:1954–1960.
30. Ames P, Galor A. Cyclosporine ophthalmic emulsions for the treatment of dry eye: a review of the clinical evidence. *Clin Investig (Lond)*. 2015;5:267–285.
31. Daull P, Barabino S, Feraille L, et al. Modulation of inflammation-related genes in the cornea of a mouse model of dry eye upon treatment with cyclosporine eye drops. *Curr Eye Res*. 2019;44:476–485.
32. European Medicines Agency. Ikervis EPAR. https://www.ema.europa.eu/en/documents/product-information/ikervis-epar-product-information_en.pdf; 2023. Accessed March 28, 2023.
33. Butovich IA, Lu H, McMahon A, Eule JC. Toward an animal model of the human tear film: biochemical comparison of the mouse, canine, rabbit, and human meibomian lipidomes. *Invest Ophthalmol Vis Sci*. 2012;53:6881–6896.
34. Masoudi S. Biochemistry of human tear film: a review. *Exp Eye Res*. 2022;220:109101.
35. Chan TCY, Chow SSW, Wan KHN, Yuen HKL. Update on the association between dry eye disease and meibomian gland dysfunction. *Hong Kong Med J*. 2019;25:38–47.
36. Sassa T, Tadaki M, Kiyonari H, Kihara A. Very long-chain tear film lipids produced by fatty acid elongase ELOVL1 prevent dry eye disease in mice. *FASEB J*. 2018;32:2966–2978.
37. Sawai M, Watanabe K, Tanaka K, et al. Diverse meibum lipids produced by Awat1 and Awat2 are important for stabilizing tear film and protecting the ocular surface (vol 24, 102478-1. e18, 2021). *iScience*. 2021;24:102478.
38. FDA. *Restasis (cyclosporine) ophthalmic label*; 2012. https://www.accessdata.fda.gov/drugsatfda_docs/label/2012/050790s020lbl.pdf. Accessed November 9, 2023.